Photocurrent-Determining Processes in Quasi-Solid-State Dye-Sensitized Solar Cells Using Ionic Gel Electrolytes

Wataru Kubo,[†] Shingo Kambe,[†] Shogo Nakade,[†] Takayuki Kitamura,[†] Kenji Hanabusa,[‡] Yuji Wada,[†] and Shozo Yanagida*,[†]

Material and Life Science, Graduate School of Engineering, Osaka University, Suita 565-0871, Japan, and Graduate School of Science and Technology, Shinshu University, Ueda 386-8567, Japan

Received: January 30, 2003; In Final Form: February 28, 2003

Dye-sensitized solar cells (DSCs) using ionic liquids, 1-alkyl-3-methylimidazolium iodide (alkyl: C_3-C_9), were fabricated with and without a low molecular weight gelator. The highest energy conversion efficiency of 5.0% was obtained from a quasi-solid-state DSC using 1-hexyl-3-methylimidazolium iodide (HMImI). Gelation of these ionic liquids demonstrated better high-temperature durability without decreasing the solar cell efficiency. However, the short-circuit currents (J_{SC}) obtained from these DSCs were about 70% of that obtained from DSCs using organic liquid electrolyte (OLE). To explain the difference of the J_{SC} values between the DSCs using ionic liquid electrolyte (ILE) and OLE, four primitive processes in DSCs, that is, charge transport in the electrolytes, light absorption by I_3^-, electron diffusion in a TiO_2 electrode, and charge recombination, were examined. Viscosities of the ILE decreased with increasing I_3^- concentration and alkyl chain length. In ILE, measured J_{SC} values increased with increasing I_3^- concentration up to 0.7−1.4 M, depending on the alkyl chain length. Measured J_{SC} values showed the same tendency as that estimated using a calculation with a model in which the redox couple is transported by diffusion in electrolytes. These results suggest that the slower diffusion of I_3^- to the counter electrode (CE) limits the J_{SC} values and requires a larger amount of I_3^- in ILE. However, increasing [I_3^-] to more than 0.7−1.4 M resulted in the decrease of J_{SC}. At the optimized concentration of I_3^- in ILE, the influence of the absorption was estimated to be 13% of the decrease on photocurrent. To the estimate electron diffusion length in the TiO_2 electrode, the electron diffusion coefficient (D_e) and electron recombination lifetime (τ) were measured, showing faster D_e and shorter τ in ILE than in OLE. The faster D_e was caused by the higher concentration of cation in ILE. However, the shorter τ was caused by the higher concentration of I_3^- and depended on the concentration. Thus, the electron diffusion lengths (L) in the DSC using ILE were shorter than that using OLE. Their shorter L also reduced the J_{SC} in the ILE and with the increase of I_3^- concentration. Among the ILE, the increase of alkyl chain length increased τ. This result should explain the highest efficiency observed in HMImI. During the durability test of the DSC at high temperature, a decrease of the efficiency of the cell using ILE was observed in 1000 h. Time course change of I_3^- concentration measurements revealed that the gelation of the electrolyte depresses a decrease of I_3^- concentration caused by sublimation of I_2. Depression of sublimation of I_2 is important to improve the high-temperature durability in nonvolatile ionic liquid electrolyte.

Introduction

Dye-sensitized solar cells (DSCs) have attractive features in high-energy conversion efficiency and low production cost.[1,2] Their working principle is based on the injection of electrons from photoexcited states of a dye adsorbed on an electrode to the conduction band of the semiconductor followed by the reduction of the oxidized dye with a charge mediator.[3] Figure 1 illustrates the geometry and these processes in an energy diagram of a DSC. In this system, the large surface area of the nanoporous electrode enables us to generate high photocurrent up to 20 mA cm^{-2}.[4] To fill a hole transport material in the porous electrode, organic solvents containing redox electrolytes (OLEs) have been employed as mediators. This configuration requires robust sealing to avoid leakage, evaporation, and contamination of the solvent.[5] Several attempts have been made to substitute the liquid electrolyte by solid materials, such as inorganic[6−8] or organic[9−13] hole transport materials, and polymer electrolyte.[14] However, DSCs using these solid materials have been showing lower efficiency than those of DSCs using liquid electrolyte. This is mostly because of the insufficient penetration of the solid materials into the nanoporous electrode and/or of fast charge recombination in DSCs. In comparison to these attempts, gel electrolytes containing I^-/I_3^- redox couples and organic liquid (OGEs) seem to present better efficiency than the others.[15−20] From a practical point of view, however, the presence of organic solvents in gel electrolytes will cause problems such as high-temperature instability and flammability.[5]

Room-temperature ionic liquids have attractive features in chemical stability, nonvolatility, nonflammability, and wide electrochemical window. Recently, several studies about DSCs using ionic liquid electrolytes (ILEs) were reported.[21−26] We reported DSCs with an ILE and an ionic gel electrolyte (IGE) based on an ionic liquid and a low molecular weight gelator.[23] The DSCs using ILE and IGE showed better high-temperature durability than those using OLE due to nonvolatility of the ionic

* E-mail: yanagida@mls.eng.osaka-u.ac.jp.
[†] Osaka University.
[‡] Shinshu University.

10.1021/jp034248x CCC: $25.00
Published on Web 04/11/2003

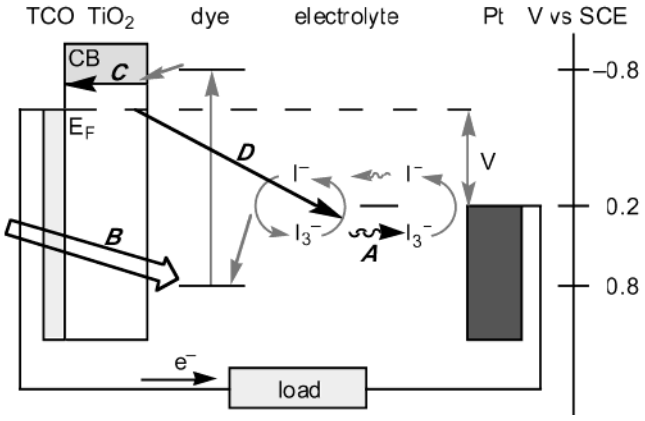

Figure 1. Schematic description of a dye sensitized TiO_2 solar cell, including the energy conversion processes: (A) diffusion of I_3^- in electrolyte; (B) absorption of the incident light by I_3^- in electrolytes; (C) diffusion of electrons in the conduction band of TiO_2 to TCO; (D) charge recombination between injected electrons and I_3^- in electrolyte.

TABLE 1: *I*−*V* Characteristics of Solar Cells with Different Electrolytes[a]

electrolyte	area/cm^2	V_{OC}/V	J_{SC}/mA cm^{-2}	FF	η/%
OLE	0.24	0.72	16.6	0.67	7.9
OGE	0.24	0.75	14.5	0.68	7.4
ILE	0.27	0.64	11.8	0.66	5.0
IGE	0.27	0.64	11.8	0.67	5.0

[a] All samples were measured under AM1.5, 100 mW cm^{-2} irradiation.

liquid.[23] However, the use of the ILE caused the decrease of J_{SC} in comparison with the case of IGE. The highest J_{SC} that we have obtained for ILE or IGE under AM1.5, 100 mW cm^{-2} irradiation, was 11.8 mA cm^{-2}, which was about 70% of the value obtained from OLE. Table 1 (recalled from ref 23) summarizes the characteristics of these solar cells.

The factors determining photocurrents were not perfectly understood, but the following reasons can be considered mainly. For charge transport in electrolyte (path A in Figure 1), the viscosity of the electrolyte affects J_{SC} significantly.[27] The ionic liquids, 1-alkyl-3-methylimidazolium iodide used here, showed much higher viscosities than organic solvents.[23] To compensate the slow diffusion of I_3^- caused by the high viscosity of ILE, higher concentration of I_3^- was required.[21,23] The increase of the I_3^- concentration in ILE decreases the electrolyte viscosity.[21] However, the increase of $[I_3^-]$ is not desirable due to the high absorption of UV light (path B, $\epsilon = 2.55 \times 10^4$ M^{-1} cm^{-1} at 360 nm, 3.88×10^4 M^{-1} cm^{-1} at 291 nm in acetonitrile),[28] whose tail extends into the visible range (>500 nm). Light absorbed by I_3^- was not used to excite electrons in the dyes. Consequently, the J_{SC} values of the solar cells were decreased.[21] Hence, each effect of the viscosity and I_3^- concentration on J_{SC} should be ruled out for further understanding and optimization. For this purpose, viscosity, conductivity, absorption spectra of electrolytes, and incident photon to current efficiency (IPCE) were measured.

In DSCs, electrons in the TiO_2 electrode are surrounded by cations in the nanoscale range. This has led to the interpretation of the electron transport in nanoporous TiO_2 films (path C) with ambipolar diffusion.[29] Our group reported the increase of electron diffusion coefficients (D_e) with increasing concentration of cations,[30,31] including imidazolium cation.[31] ILE contains about 10 times as much imidazolium cation as OLE, which leads to an increase of electron diffusion coefficients in TiO_2 filled by ILE compared to OLE.

CHART 1: Chemical Structures of (a) 1-Alkyl-3-methylimidazolium Iodide and (b) Gelator

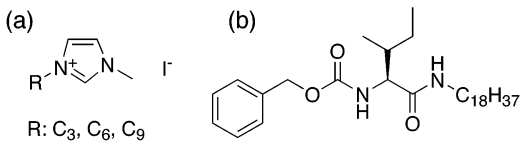

To take out most of the photogenerated electrons to the external circuit, the diffusion length, expressed as the square root of the product of D_e and the lifetime (τ) of charge recombination, which occurs between electrons in TiO_2 and I_3^- (path D), must be longer than the thickness of the TiO_2 film. To obtain high enough L, adequate τ is required.[32,33] However, τ in ILE may be lowered due to the high concentration of I_3^-. To substantiate this, electron diffusion coefficients and recombination lifetimes were measured with various ionic liquids and I_3^- concentrations.

The ionic conductivity of 1-alkyl-3-methylimidazolium iodides (C_3−C_9) decreased with increasing alkyl chain length.[23] However, the imidazolium with a hexyl group showed the highest conversion efficiency.[23] This result could not be explained only by charge transport properties of ILE. The measurements of D_e and τ in various ILE explained the result, and then this was also discussed.

In heat tests at 85 °C, IGE exhibited no decrease of conversion efficiency in 1000 h,[23] while the cell using ILE showed a decrease of that. To explain the better durability observed in IGE, two possibilities, the depression of dye desorption and the decrease of I_3^- concentration, were also investigated.

Experimental Section

Sample Preparation. 1-Alkyl-3-methylimidazolium iodides (Chart 1a, alkyl = propyl (PMImI), hexyl (HMImI), nonyl (NMImI)) were synthesized from 1-methylimidazolium (Nacalai Tesque) and the corresponding alkyl iodide (Tokyo Chemical Industry). The details of the synthesis were described in section 1 of the Supporting Information. The ILEs were prepared by mixing I_2 with 1-alkyl-3-methylimidazolium iodide. A gelator (Chart 1b) was synthesized as reported previously.[34] This gelator forms thermoreversible physical gels in a variety of liquids at very low concentration without losing ionic conductivity.[35] IGEs for DSCs were prepared by mixing 40 g L^{-1} of the gelator with ILE, followed by heating at 130 °C to dissolve the gelator. As a reference, all OLEs used in this report were prepared by dissolving 0.6 M 1,2-dimethyl-3-propylimidazolium iodide (DMPImI: Shikoku Corp.), 0.1 M I_2, 0.05 M LiI, and 1 M 4-*tert*-butylpyridine in methoxyacetonitrile.

Transparent nanocrystalline TiO_2 films were prepared as follows. A TiO_2 paste (Nanoxide-T, Solaronix) was deposited on a conducting glass substrate (F-doped SnO_2, sheet resistance 10 Ω square^{-1}, Nippon Sheet Glass), followed by sintering at 550 °C for 30 min in air. A light scattering layer used in a previous report[23] was not used in this report to simplify the discussions about the light absorption. The resulting TiO_2 films ($w = 10$ μm) were cut into pieces with suitable size and heated again at 450 °C for 15 min. After cooling to 130 °C, the films were immersed in a 5.0×10^{-4} M *cis*-dithiocyanate-*N*,*N*′-bis-(4-carboxylate-4-tetrabutylammoniumcarboxylate-2,2′-bipyridine) ruthenium(II) (N719, Ruthenium TBA 535, Solaronix) in acetonitrile/2-methyl-2-propanol = 1/1 solution for 24 h. The resulting electrodes were rinsed with acetonitrile. After drying at room temperature, the porous electrode was covered by a Pt sputtered conducting glass (F-doped SnO_2 sheet resistance 10

Ω square^{-1}, Asahi Glass) as a counter electrode (CE). The gap between two electrodes was sealed by thermal adhesive films (HIMILAN 1652, Mitsui-Dupont Polychemical, thickness = 50 μm). Melted gel electrolyte was injected from a hole made on the counter electrode while temperature was kept constant at 100 °C. The hole was sealed with a cover glass (Iwaki Glass), HIMILAN film, and resin (Torr Seal, Varian Vacuum Products).

Measurements. Photoenergy conversion efficiency was evaluated using an AM1.5 solar simulator (YSS-50A, Yamashita Denso) and a PC controlled voltage current source/meter (R6246, Advantest) at 25 °C. We adapted the solar simulator to the Japanese Industrial Standard for amorphous solar cells in the cell efficiency determination.[36] The intensities of incident light dependent short-circuit currents were examined, where the intensity was controlled by an optical lens and neutral density filters with a H_2O filter to avoid heating of DSCs by IR light. Incident photon to current efficiency (IPCE) measurements were carried out using a commercial setup for IPCE measurement (PV-25DYE, JASCO) under 5 mW cm^{-2} monochromatic light illuminations. All measured IPCE values were not corrected for the loss of incident light due to the absorption and reflection by the conducting glass support. Conductivity of electrolytes was determined by ac impedance measurements using a two-electrode thin-layer cell.[19] Viscosity was measured with a viscometer (TVE-20H, Toki Sangyo) with a temperature controller (R-134A, Neslab Instruments) at 25 ± 0.1 °C. Film thickness was determined using a surface profiler (Dektak 3, Sloan). The morphology of the interface between SnO_2:F conducting glass and TiO_2 was studied with a scanning electron microscope (SEM, JSM 6700F, JEOL) equipped with an energy dispersive spectrometer (EDS, JED 2200, JEOL). Raman spectra of electrolytes were measured with a Raman spectrometer (spectrum GX2000R, Perkin-Elmer) equipped with a Nd:YAG laser (10−1600 mW). Electron diffusion coefficients in the TiO_2 electrode were measured by transient photocurrent induced by a laser pulse (INDI Series Pulsed Nd:YAG Lasers, Quanta-Ray, pulse width 7 ns, λ = 532 nm) in the presence of continuous background illumination (He:Ne laser, Melles Griot, λ = 632.8 nm). The theory of the measurement[37] and details of the experiment[38] were documented elsewhere. This measurement was performed with a DSC whose TiO_2 electrode thickness was 5.5 ± 0.5 μm.

Electron recombination lifetimes were measured by intensity modulated photovoltage spectroscopy (IMVS). The theory of the measurement[39] was documented elsewhere. The intensity of a diode laser (Lablasers, Coherent, λ = 635 nm) was modulated with a frequency range from 500 to 0.01 Hz. The light intensity was controlled by neutral density filters. The open-circuit voltage responses to the modulated light were amplified by a differential amplifier (5307, NF Electronic Instruments), and the amplitude and phase shift of the signals were monitored with a LCR meter (3522 LCR Hitester, Hioki).

For these measurements above, we employed a DSC using ILE without gelator. We discussed the difference of J_{SC} with the DSCs using ILE and OLE. Since the DSC using IGE showed identical photocurrent−voltage properties to those of the cell using ILE and the gelator formed gel electrolyte without losing ionic conductivity[19,35] and decreasing IPCE,[19] we consider that these discussions based on the results of ILEs are applicable to the DSC with the gelator.

For heat tests, the cells were stored in a thermostat at 85 °C for 1000 h.[40] The time course change of I_3^- concentration was determined by the absorbance of electrolyte. The time course change of the amount of adsorbed dye on a TiO_2 electrode was determined by the previously reported procedure.[2]

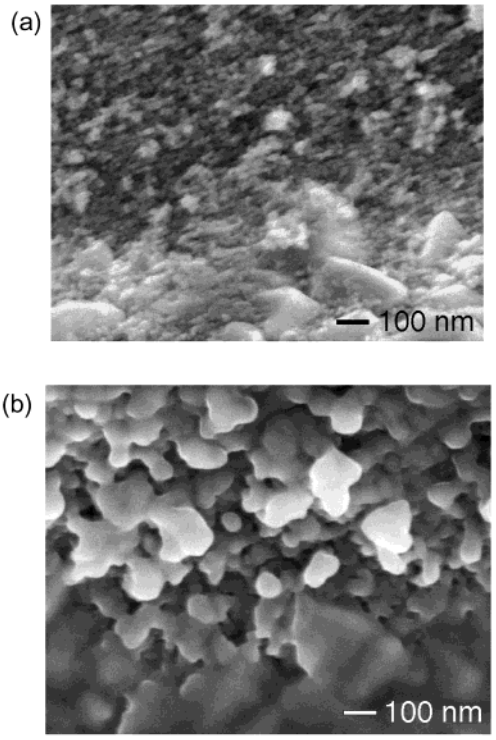

Figure 2. Scanning electron micrographs of the cross section of DSC (a) before and (b) after introduction of IGE at the interface between TiO_2 and the SnO_2:F layer.

Results and Discussion

Penetration of IGE into a Porous TiO_2 Electrode. Figure 2a shows the cross section of the interface between TiO_2 and the SnO_2:F layer of conducting glass before introduction of IGE. Small TiO_2 particles (upper layer, diameter = 18 nm) formed a nanosized pore and made good contact with the SnO_2 particle (lower layer, diameter = 300 nm). Figure 2b shows the interface after introduction of IGE. Tens nanometer sized TiO_2 particles could not be seen clearly, but larger spheres were observed. The result of EDS analysis (section 2 of the Supporting Information) in the same area of Figure 2b showed the apparent existence of the element I, which was not observed in that of Figure 2a. These results support that IGE penetrated well into the porous TiO_2 electrode deep into the SnO_2:F layer of conducting glass and filled the complete pores.

Charge Transport in Electrolytes. Figure 3 shows the effect of I_3^- concentration on viscosity and conductivity of imidazolium iodides. I_3^- was formed by addition of I_2 to the imidazolium iodides. Increases of conductivity and decreases of viscosity with increasing I_3^- concentration were observed. The increases of viscosity of ILEs with alkyl chain length observed here can be explained with their van der Waals force.[23,41] The decreases of viscosity with increasing I_3^- concentration are probably explained as follows. Generally, ionic liquids that consist of larger anions exhibit lower viscosity by strong delocalization of the negative charge.[41] In the electrolyte used here, larger anions, such as I_3^-, were formed. These anions probably decreased the viscosity of the electrolytes.

Figure 4 shows the influences of I_3^- concentration on J_{SC} measured under AM1.5, 100 mW cm^{-2} irradiance. All ILEs showed increases of J_{SC} with the increase of I_3^- concentration at low I_3^- concentration range. This tendency could be explained

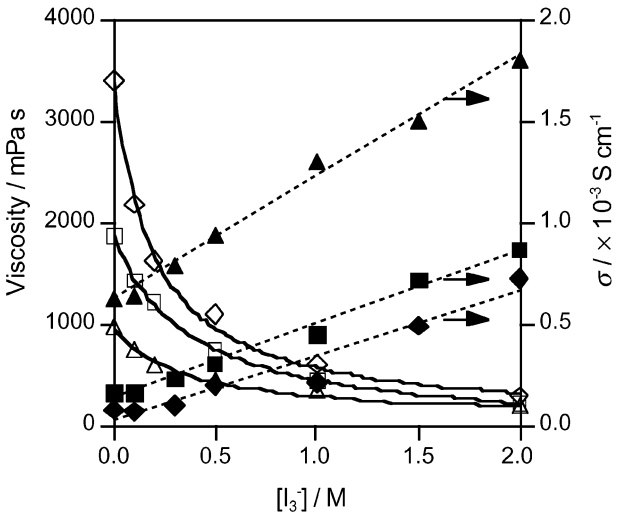

Figure 3. Effect of I_3^- concentration in ILE on viscosity (left axis; open triangle, PMImI; open square, HMImI; open diamond, NMImI) and conductivity (right axis; closed triangle, PMImI; closed square, HMImI; closed diamond, NMImI) measured at 25 °C.

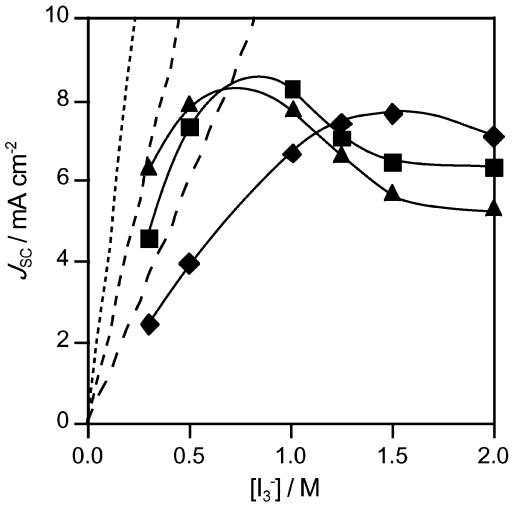

Figure 4. Effect of I_3^- concentration on J_{SC} from DSC (area = 0.25 cm^2) using ILE. Measured values are plotted by closed triangles for PMImI, closed squares for HMImI, and closed diamonds for NMImI. Calculated J_{SC} values from eq 1 are shown by the dotted curve for PMImI, the short dashed curve for HMImI, and the long dashed curve for NMImI. All J_{SC} values were measured under AM1.5, 100 mW cm^{-2} irradiation.

with the I_3^- concentration gradient in DSCs produced by slow diffusion of I_3^-. Papageorgiou et al. derived equations which represent the photocurrent being limited by the diffusion of I_3^- with an assumption that photoelectrons are generated homogeneously through the entire thickness of the electrodes. The limiting current is expressed as[27]

$$J_{lim} = 6PFD_{I_3^-}C/w \quad (1)$$

where P is porosity, F is Faraday's constant, $D_{I_3^-}$ is the diffusion coefficient of I_3^-, C is the initial concentration of I_3^-, and w is the film thickness. Photocurrents calculated with eq 1 were also shown in Figure 4. The constants used in the calculation were measured thickness ($w = 10\ \mu m$); estimated diffusion coefficient ($D_{I_3^-}$), using the reported value ($D_{I_3^-} = 9.0 \times 10^{-8}$ cm^2 s^{-1} in neat HMImI)[27] and measured viscosity described in Figure 3; and porosity ($P = 0.42$). The porosity of the dyed film was calculated using the measured porosity of bare TiO_2 films

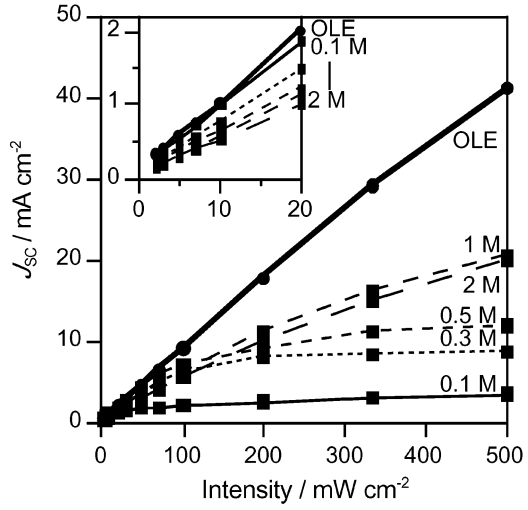

Figure 5. Effect of incident light intensity on J_{SC} of DSC (area = 0.25 cm^2) using OLE (circles) and ILE (HMImI, squares) with various I_3^- concentrations: 2 M (long dashed curve); 1 M (dashed curve); 0.5 M (short dashed curve); 0.3 M (dotted curve); 0.1 M (solid curve).

(=0.60) and a 30% decrease caused by the change of morphology due to dye adsorption.[42] The calculated J_{SC} values showed the same order as that of the J_{SC} values observed in the measurements at the low I_3^- concentration range. This agreement suggests that the J_{SC} was limited by the transport of I_3^- to the counter electrode.

The calculated J_{SC} values in the low I_3^- concentration range were about 50% for PMImI and 30% for HMImI and NMImI higher than the measured values. These discrepancies of J_{SC} were probably caused by the following two reasons. First, the diffusion of I_3^- in a DSC was obstructed by the structure of the nanoporous electrode. The $D_{I_3^-}$ in a nanoporous film immersed in acetonitrile exhibited smaller values than that in bulk electrolyte.[43] Second, eq 1 was derived with the assumption that the absorption of a dye-coated photoelectrode was sufficiently small to produce I_3^- constantly by reduction of oxidized dye across the film, but in practical DSCs, incident light was mostly absorbed by dyes on a nanoporous electrode a few microns from the transparent conductive oxide (TCO) side. For example, the calculation, using eq 4 with light absorption shown in Figure 6 and described later, exhibited that 50% of the incident light was absorbed in the range of 2.4 μm. Hence, the rate of generation of I_3^- should be higher at the TCO side and lower at the CE than calculated. This would explain the lower values of observed J_{SC} than calculated J_{SC}.

To support that the J_{SC} was limited by the I_3^- transport, J_{SC} was measured in the cells with various thickness of additional electrolyte layer. This can allow us to measure the effect of I_3^- under the same condition of incident light absorption by I_3^- and charge recombination in the DSCs with different I_3^- transport length. The limiting current with the additional electrolyte layer was expressed as[27]

$$J_{lim\,a} = J_{lim}\frac{1 + \frac{b}{lP}}{1 + 3P\frac{b}{l} + \left(\frac{b}{l}\right)^2} \quad (2)$$

where b is the thickness of the additional electrolyte layer. According to this equation, the limiting current decreases with increasing thickness of the electrolyte layer. Measured J_{SC} values for OLE and ILE were shown in Table 2. The J_{SC} values were measured under AM1.5, 100 mW cm^{-2} adsorption with various

TABLE 2: Effect of Additional Electrolyte Layer Thickness on J_{SC}[a]

thickness/μm		0	10	40
J_{SC}/(mA cm^{-2})	OLE	13.3	12.8	12.3
	ILE	9.4	7.2	5.9

[a] All J_{SC} values were measured under AM1.5, 100 mW cm^{-2} irradiation. Sample area = 0.25 cm^2.

thicknesses of the electrolyte layer (0−40 μm). In OLE, the J_{SC} showed little decrease. This agrees with the observation that the J_{lim} in OLE was much higher than the experimentally obtained J_{SC} from OLE, and the electrolyte thickness did not affect on the J_{SC}. In ILE, the experimental result of the J_{SC} was limited by the I_3^- concentration and affected by the increase of the thickness as described by eq 2.

Figure 5 shows J_{SC} values measured at light intensities between 1 and 500 mW cm^{-2}. In OLE, J_{SC} increased linearly with light intensity, because the low viscosity of the organic solvent allowed sufficient charge transport of I_3^- with high $D_{I_3^-}$. In the case of ILE (HMImI) with low I_3^- concentration ($\leq$0.5 M), J_{SC} did not increase with light intensity linearly because of their low I_3^- transport ability discussed previously. J_{SC} values under various light intensities were also measured for PMImI and NMImI. PMImI showed better linearity in the increase of J_{SC} than the other two ILEs. This linearity can be explained by the relatively faster I_3^- diffusion.

Absorption of Incident Light by I_3^-. To compensate the slow diffusion of I_3^- to the CE, the ILE cells required higher initial concentration of I_3^- than the OLE cell. High concentration of I_3^- also decreased the viscosity of the ILE to achieve better mass transport of I_3^-. However, I_3^- in the electrolytes absorbs light strongly. Thus, the absorption of incident light by I_3^- should be taken into account in the ILE cells. Figure 6 shows absorption spectra of ILE ([I_3^-] = 1 M), OLE ([I_3^-] = 0.05 M), and dye adsorbed TiO_2. Absorbance of these spectra was normalized to the values corresponding to 1 μm thickness of these, using absorption coefficients of dye or I_3^- (ϵ_{dye} = 1.26 × 10^4 M^{-1} cm^{-1} at 530 nm, $\epsilon_{I_3^-}$ = 2.55 × 10^4 M^{-1} cm^{-1} at 360 nm[28]). As it is seen, I_3^- absorbed near UV to visible light strongly, and the tail of this absorption band extended over 500 nm. Figure 7a shows IPCE spectra of DSCs using OLE and ILE. IPCE is defined as the number of generated electrons divided by the number of incident photons.[2] A strong dip of the IPCE spectra observed around 380 nm in ILE should be attributed to the absorption of I_3^- in ILE, because the wavelength was identical to that of the peak of the absorption spectrum of ILE. IPCE values for all ILEs were lower than that of OLE at the entire range of wavelength because of not only the absorption of I_3^- but also other factors such as charge recombination discussed later. We tried to extract the effect of light absorption by I_3^- on J_{SC} from the following estimation. The IPCE spectra for ILE were normalized to OLE by using the IPCE value at 550 nm, where the absorption of I_3^- was negligible. As shown in Figure 7b, the normalized IPCE spectra for ILE showed excellent agreement with that of OLE at the longer wavelength range (>550 nm). J_{SC} and IPCE have the following relationship.[44]

$$J_{SC} = \int qF(\lambda)[1 - r(\lambda)]\mathrm{IPCE}(\lambda)\,\mathrm{d}\lambda \qquad (3)$$

where q is the electron charge, $F(\lambda)$ is the incident photon flux density at wavelength λ, and $r(\lambda)$ is the incident light loss of light intensity due to absorption and reflection by the conducting glass support. With the normalized IPCE and AM1.5 photon flux described in Figure 6 (right axis),[45] the calculated J_{SC} values were 12.7 mA cm^{-2} for OLE, 11.0 mA cm^{-2} for PMImI, 10.9 mA cm^{-2} for HMImI, and 11.0 mA cm^{-2} for NMImI. As a result, the decrease of J_{SC} caused by absorption of I_3^- in ILE was estimated to be 13%.

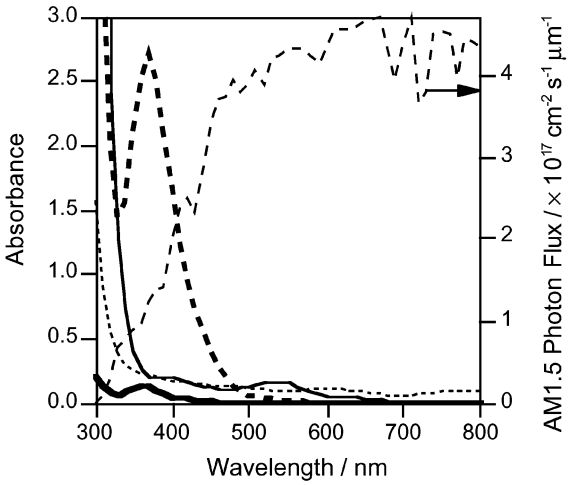

Figure 6. Absorption spectra of OLE [I_3^-] = 0.05 M (bold curve), ILE [I_3^-] = 1 M (bold dashed curve), and dye adsorbed TiO_2 film (solid curve) normalized to 1 μm thick, conducting glass (dotted curve); and AM1.5 photon flux density (dashed curve, right axis).

To explain the dip of IPCE caused by light absorption quantitatively, light-harvesting efficiency (LHE), that is, the ratio of the number of photons absorbed by the dye-adsorbed TiO_2 film to that of incident photons, was estimated. With the Lambert−Beer law and a model in which a cell is constructed with a series of dye-adsorbed TiO_2 film layers and electrolyte layers that have infinitesimal thickness, the LHE is given by[46]

$$\mathrm{IPCE}(\lambda) = [1 - 10^{-(A_D(\lambda)+A_E(\lambda)P)}]\left(\frac{A_D(\lambda)}{A_D(\lambda) + A_E(\lambda)P}\right) \qquad (4)$$

where $A_D(\lambda)$ is the absorbance of the dye-adsorbed TiO_2 film, $A_E(\lambda)$ is the absorbance of the electrolyte that has the same thickness as that of the TiO_2 film, and P is porosity. LHE values for OLE and ILE shown in Figure 7b were calculated from the absorbance of the dye and the electrolytes, the transmittance of conducting glass in Figure 6, and film geometry (w = 10 μm, P = 0.42). The calculated LHE for OLE showed good agreement with the observed IPCE, while the calculated LHE for ILE did not agree around the dip. This disagreement for ILE could be explained by the decrease of the I_3^- concentration. I_3^- in electrolyte should be consumed for the formation of higher polyiodide species, such as I_5^-, I_7^-, and I_9^- (i.e. $2I_3^- \rightarrow I_5^- + I^-$). Higher polyiodides show similar shape of absorption spectra and absorption coefficient to I_3^- (for example, $\epsilon_{I_9^-}$ = 2.61 × 10^4 M^{-1} cm^{-1} at 365 nm).[47] We observed the existence of higher polyiodide species in ILE by a peak around 150 cm^{-1} in Raman spectra (data not shown), which were similar to those of the previous report.[48] Hence, the total absorbance of the electrolyte should be decreased.

The electron injection yield from dye to TiO_2 might also lower the J_{SC} besides the discussions above. Here we evaluated the products of the electron injection efficiency and charge collection efficiency in OLE and ILE. The IPCE and the product are related by[2]

$$\mathrm{IPCE}(\lambda) = \mathrm{LHE}(\lambda)\phi_{inj}\eta_C \qquad (5)$$

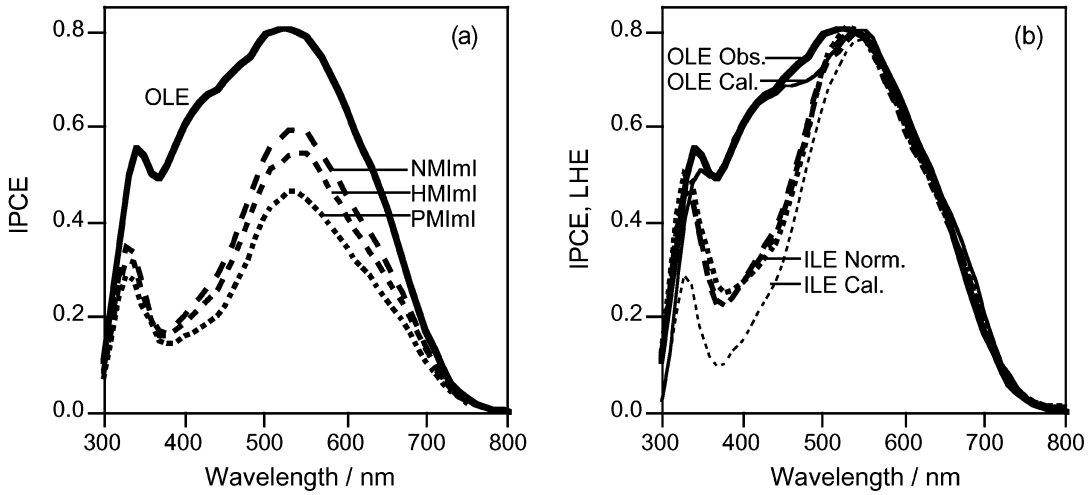

Figure 7. (a) Observed IPCE spectra of DSC (area = 0.25 cm^2) with OLE (bold solid curve) and ILE containing 1 M I_3^- (PMImI, dotted curve; HMImI, short dashed curve; NMImI, long dashed curve). (b) IPCE observed for OLE (bold solid curve), IPCE for ILE normalized at 550 nm (PMImI, dotted curve; HMImI, short dashed curve; NMImI, long dashed curve), and calculated LHE for OLE (thin solid curve) and ILE (thin dotted curve).

where ϕ_{inj} is the electron injection yield and η_C is the charge collection efficiency. For OLE, the IPCE exceeded 80% in the wavelength range 520−530 nm, as shown in Figure 7a. The transmittance of the conducting glass support (shown in Figure 6) was about 80% in this wavelength range. The results show that IPCE, taking into account the transmittance of TCO, is close to 100%. This leads to ϕ_{inj} and η_C being almost unity, which was in good agreement with the previous report.[2] To assess the products in ILE, we compare the J_{SC} values from DSCs using ILE and OLE containing low I_3^- concentration. The inset of Figure 5 showed the expansion of the intensity up to 20 mW cm^{-2}. In the intensity region, J_{SC} increased linearly with light intensity for OLE and ILE containing low I_3^- concentration. This linearity indicates that I_3^- transport does not limit the J_{SC}. ILE with low I_3^- concentration (0.1 M) showed identical J_{SC} to that of OLE at irradiance under 10 mW cm^{-2}. This suggests that the products of ϕ_{inj} and η_C for DSCs using ILE are also unity at these conditions.

Electron Diffusion in the TiO_2 Electrode. The electron diffusion coefficient in the nanoporous TiO_2 electrode was estimated using the τ_C, which was obtained by the fitting thetransient photocurrent decay with $\exp(-t/\tau_C)$,[37]

$$D_e \approx \frac{w^2}{2.35\tau_C} \tag{6}$$

where w is the TiO_2 film thickness. Measured electron diffusion coefficients as a function of J_{SC} are plotted in Figure 8. The measurements were repeated several times on several samples. Each plot of the D_e was the average of these. All samples show a power law dependence on J_{SC}, and the slopes of the plots were comparable regardless of these electrolytes. The slope has been interpreted with the intraband charge trap density in the TiO_2 films. The comparable slopes observed here also support that the slopes are the inherence of the TiO_2 films. The D_e observed in ILE was about 3 times larger than that in OLE at the same J_{SC}. This discrepancy seems to agree with the previously reported result.[30,31] The increase of D_e with the increase of the concentration of the cation was interpreted with ambipolar diffusion, which is related with the diffusion coefficients of electrons and cations, and the concentrations of these charges. The presence of imidazolium ions in acetonitrile brought a steep increase of D_e at high ionic concentration.[31] In

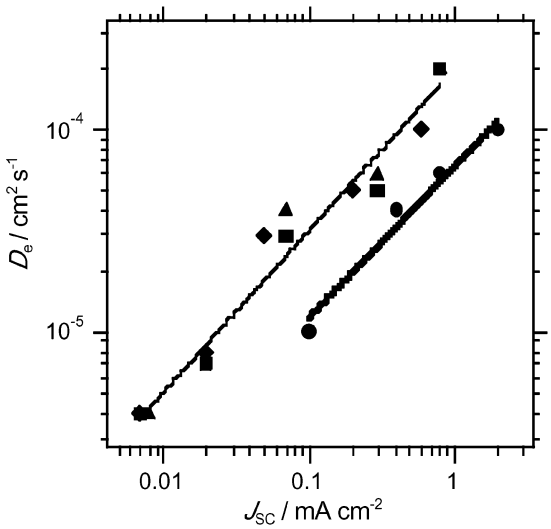

Figure 8. Electron diffusion coefficient in a TiO_2 electrode filled with various electrolytes as a function of J_{SC}, The electrolytes are OLE (circles), ILE using PMImI (triangles), HMImI (squares), and NMImI (diamonds).

ILE, the concentration of imidazolium cation was about 10 times as much as that in OLE. In ambipolar diffusion for the case of DSCs, when increasing the concentration of cations, the ambipolar diffusion coefficient approaches the diffusion coefficients of electrons in TiO_2.[29] Measured D_e in OLE should not reach the diffusion coefficient of electrons in TiO_2, because the concentration of cation in OLE was not sufficient. The concentrations of cation in these ILEs were high enough so that the measured D_e must be the diffusion coefficient of the electrons in the TiO_2 films, probably explaining the similar D_e values observed here regardless of the alky chain length.

Charge Recombination. Each of the cells using OLE and ILE showed a semicircle on a plot in the complex plain for all IMVS measurements. The electron recombination lifetime was estimated using the frequency (f), when the imaginary part of ΔV exhibited a minimum value, with $\tau = 1/(2\pi f)$.[32,33,39] Measurements were performed on the DSCs using OLE and ILE with different I_3^- concentrations. Figure 9 shows the obtained electron lifetime as a function of J_{SC}. Each plot of τ was the average of four samples, and the average deviation of

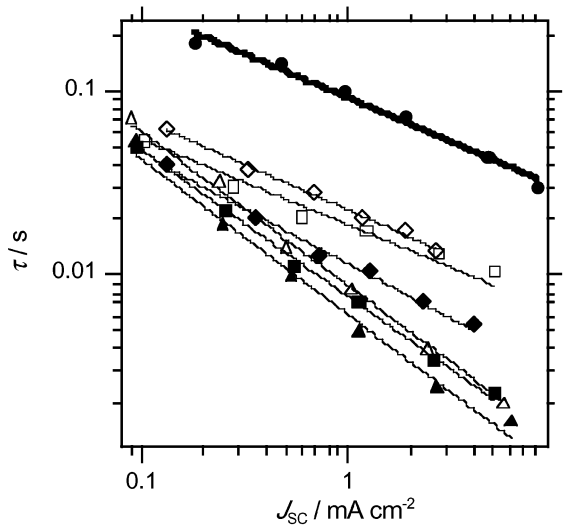

Figure 9. Dependence of electron recombination lifetime at open circuit conditions (τ) under various light intensities for various electrolytes: OLE (closed circles); ILE containing 0.5 M I_3^- (open symbols); 2 M I_3^- (closed symbols) in PMImI (triangles), HMImI (squares), and NMImI (diamonds).

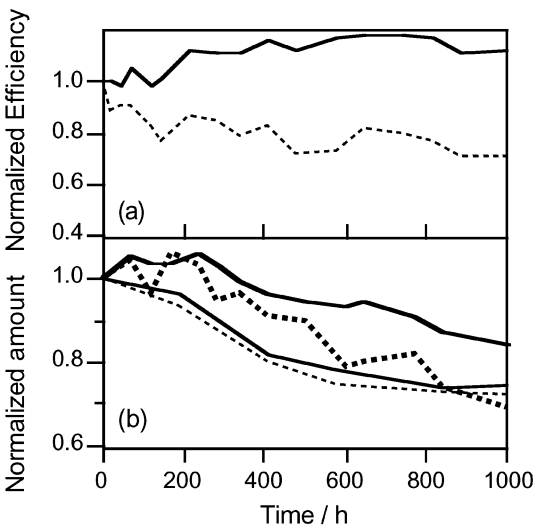

Figure 10. Time-course changes of (a) the normalized efficiency for ILE (dotted curve) and IGE (solid curve), (b) the concentration of I_3^- for ILE (bold dotted curve) and IGE (bold solid curve), and the amount of adsorbed dye for ILE (thin dotted curve) and IGE (thin solid curve).

the values was 16%. The electron lifetime in OLE was 5−30 times longer than those in ILE. The lifetime of an electron in the TiO_2 electrode should decrease with the increasing of the concentration of I_3^- in the electrolyte, because the probability of encountering electrons in the TiO_2 electrode with I_3^- increases with the increasing of [I_3^-]. Here, the concentrations of I_3^- in ILE were 10−40 times higher than those in OLE. Hence, the measured lifetimes in ILE, that were 5−30 times shorter than those in OLE, showed good agreement with the difference of the I_3^- concentration in these electrolytes. Among the same electrolytes, the increase of I_3^- concentration also resulted in the decrease of the lifetime. With the measured diffusion coefficients in ILE, the diffusion lengths[32,33] $L = (D_e\tau)^{1/2}$ in ILE were evaluated, showing shorter L than that in OLE. The shorter L caused by the high concentration of I_3^- in ILE probably lowered the charge collection efficiency in ILE.

The length of the alkyl chain of these imidazolium cations also affected the electron recombination lifetime. The lifetime increased with the increase of the alkyl chain length. This is because hydrophobic alkyl chains may impede I_3^- from reaching TiO_2. This result seems to agree with the reported cobalt polypyridine complexes as redox couple[49] or ruthenium polypyridine complexes with long alkyl chain as dye.[25,50] In Figure 4, the order of measured J_{SC} values at low I_3^- concentration, PMImI > HMImI > NMImI, can be interpreted with the same order of the viscosity of these electrolytes. At high I_3^- concentration, the order was changed to NMImI > HMImI > PMImI. These results cannot be explained only by the viscosity of electrolytes, absorption of I_3^- in the electrolytes, and D_e. At high concentration, the influence of the shorter τ should be significant. The change of the order at high I_3^- concentration would be explained by the τ, which was supported by the same order for J_{SC}.

We have reported the increase of V_{OC} with the increase of alkyl chain length of the imidazolium cation.[23] This can also be interpreted with the suppression of charge recombination by the alkyl chain of the imidazolium cations. V_{OC} values of DSCs are related to the difference between Fermi levels for electrons in the TiO_2 electrode and the redox potential of I^-/I_3^-.[51] With the same observed D_e regardless of the alkyl length, the longer recombination lifetime with the increase of alkyl chain would increase the electron density in the TiO_2 films, causing the increase of the Fermi level.

Effect of Alkyl Chain Length on Conversion Efficiency. Considering the charge transport properties, imidazolium cation with a short alkyl chain should be favorable to raise the diffusion of I_3^- in the electrolyte by its low viscosity. The low viscosity of the ILE allows lower I_3^- concentration and reduces the degree of absorption of incident light by I_3^-. The low I_3^- concentration was an advantage in their longer τ values. D_e of ILE was unchanged with the increase of alkyl chain length. But the shorter alkyl chain of imidazolium cation decreased the τ, causing the decreases of J_{SC} and V_{OC}. With a balance between the charge transport and the charge recombination in these cells, DSCs using HMImI showed the highest efficiency in the 1-alkyl-3-methylimidazolium iodides with alkyl chain length C_3−C_9.

Heat Test. In the previous paper, we reported better durability of the IGE cell at 85 °C than that of ILE cell (Figure 10a).[23] To explain the lower durability in ILE, desorption of dye molecules and decrease of [I_3^-] were measured. The time course changes of the amount of adsorbed dye and I_3^- concentration are shown in Figure 10b. The amount of adsorbed dye on the TiO_2 electrode decreased with the elapse of time until 600 h, and then it reached a constant value in both ILE and IGE. At the same time, the decrease of J_{SC} was observed only in ILE, but not in IGE. With these results from IGE, the desorbed dye should be inactive for electron injection; that is, these were physically adsorbed. This would also happen on the DSCs using ILE. On the other hand, the concentration of I_3^- in ILE was decreased by 30% from the initial concentration while it was decreased 17% in IGE. I_3^- in these electrolytes is in equilibrium with I^- and I_2, Hence, the decrease of I_3^- should be caused by the sublimation of I_2.

Conclusions

The difference of J_{SC} values between DSCs using ionic and organic liquids was well interpreted by the limitation of transport of I_3^- and high concentration of I_3^- in viscous electrolytes. Slow diffusion of I_3^- caused the lack of the local concentration of I_3^- at the counter electrode, limiting the photocurrent in ILE. Hence, high I_3^- concentration was required to compensate the low charge transport ability. However, optical absorption due

to the high concentration of I_3^- was significant in the wavelength range of <500 nm. The decrease of J_{SC} due to the absorption was estimated to be 13% in comparison with that for OLE. For electron transport properties, ILE showed about three times larger diffusion coefficients than that for OLE. This result was explained by the higher concentration of imidazolium cation. The electron lifetime was decreased with increasing concentration of I_3^- in the electrolyte. In ILE, the measured lifetime was 5−30 times shorter than that in OLE. Consequently, the electron diffusion length in DSCs using ILE was shorter than that for OLE. The shorter diffusion length would decrease the charge collection efficiency in the ILE cells. The lower photocurrents in these ionic liquids were caused by this.

The ILE having a longer alkyl chain of imidazolium cation exhibited lower I_3^- transport ability in electrolyte and longer electron recombination lifetime. With a balance between the charge transport and the charge recombination, the ILE using HMImI showed the highest efficiency in the 1-alkyl-3-methylimidazolium iodides with alkyl chain length between C_3 and C_9.

During durability tests of DSCs at 85 °C, dye desorption was observed in both ILE and IGE. The desorbed dye in ILE was probably inactive to electron injection, since the desorbed dye in IGE did not decrease the J_{SC}. After 1000 h of the test, I_3^- in ILE was decreased by 30% from the initial concentration. The degree of I_3^- decrease in ILE was larger than that in IGE, suggesting that the decrease of I_3^-, which was probably caused by the sublimation of I_2, reduced the durability of the ILE.

Acknowledgment. This work was partially supported by Grant-in-Aid for Scientific Research (No. 11358006) and Open Competition for the Development of Innovative Technology (No. 12310) in Grant-in-Aid for the Creation of Innovations through Business-Academic-Public Sector Cooperation from the Ministry of Education, Culture, Sports, Science and Technology of Japan, and the New Energy and Industrial Technology Development Organization (NEDO) under Ministry of Economy, Trade and Industry. W.K. acknowledges the Research Fellowship of Japan Society for the Promotion of Science for Young Scientists.

Supporting Information Available: Preparation of and spectral data for 1-alkyl-3-methylimidazolium iodides. This material is available free of charge via the Internet at http://pubs.acs.org.

References and Notes

(1) O'Regan, B.; Grätzel, M. *Nature* **1991**, *353*, 737.
(2) Nazeeruddin, Md. K.; Kay, A.; Rodicio, I.; Hamphry-Baker, R.; Müeller, E.; Liska, P.; Vlachopoulos, N.; Grätzel, M. *J. Am. Chem. Soc.* **1993**, *115*, 6382.
(3) Hagfeldt, A.; Grätzel, M. *Acc. Chem. Res.* **2000**, *33*, 296.
(4) Nazeeruddin, Md. K.; Péchy, P.; Renouard, T.; Zakeeruddin, S. M.; Humphry-Baker, R.; Comte, P.; Liska, P.; Cevey, L.; Costa, E.; Shklover, V.; Spiccia, L.; Deacon, G. B.; Bignozzi, C. A.; Grätzel, M. *J. Am. Chem. Soc.* **2001**, *123*, 1613.
(5) Kay, A.; Grätzel, M. *Sol. Energy Mater. Sol. Cells* **1996**, *44*, 99.
(6) Kumara, G. R. A.; Konno, A.; Shiratsuchi, K.; Tsukaraha, J.; Tennakone, K. *Chem. Mater.* **2002**, *14*, 954.
(7) Tennakone, K.; Senadeera, G. K. R.; Silva, D. B. R. A. D.; Kottegoda, I. R. M. *Appl. Phys. Lett.* **2000**, *77*, 2367.
(8) O'Regan, B.; Schwartz, D. T.; Zakeeruddin, S. M.; Grätzel, M. *Adv. Mater.* **2000**, *12*, 1263.
(9) Thelakkat, M.; Hagen, J.; Haaer, D.; Schmidt, H.-W. *Synth. Met.* **1999**, *102*, 1125.
(10) Krüger, J.; Plass, R.; Cevey, L.; Piccirelli, M.; Grätzel, M.; Bach, U. *Appl. Phys. Lett.* **2001**, *79*, 2085.
(11) Kitamura, T.; Maitani, M.; Matsuda, M.; Wada, Y.; Yanagida, S. *Chem. Lett.* **2001**, 1054.
(12) Gebeyehu, D.; Brabec, C. J.; Sariciftci, N. S.; Vangeneugden, D.; Kiebooms, R.; Vanderzande, D.; Kienberger, F.; Schindler, H. *Synth. Met.* **2002**, *125*, 279.
(13) Senadeera, G. K. R.; Jayaweera, P. V. V.; Perera, V. P. S.; Tennakone, K. *Sol. Energy Mater. Sol. Cells* **2002**, *73*, 103.
(14) Nogueira, A. F.; Paoli, M. A. D.; Montanari, I.; Monkhouse, R.; Nelson, J.; Durrant, J. R. *J. Phys. Chem. B* **2001**, *105*, 7517.
(15) Cao, F.; Oskam, G.; Searson, P. C. *J. Phys. Chem.* **1995**, *99*, 17071.
(16) Tennakone, K.; Senadeera, G. K. R.; Perera, V. P. S.; Kottegoda, I. R. M.; De Silva, L. A. A. *Chem. Mater.* **1999**, *11*, 2474.
(17) Matsumoto, M.; Wada, Y.; Kitamura, T.; Shigaki, K.; Inoue, T.; Ikeda, M.; Yanagida, S. *Bull. Chem. Soc. Jpn.* **2001**, *74*, 387.
(18) Kubo, W.; Murakoshi, K.; Kitamura, T.; Wada, Y.; Yanagida, S. *Chem. Lett.* **1998**, 1241.
(19) Kubo, W.; Murakoshi, K.; Kitamura, T.; Yoshida, S.; Haruki, M.; Hanabusa, K.; Shirai, H.; Wada, Y.; Yanagida, S. *J. Phys. Chem. B* **2001**, *105*, 12809.
(20) Murai, S.; Mikoshiba, S.; Sumino, H.; Hayase, S. *J. Photochem. Photobiol. A: Chem.* **2002**, *148*, 33.
(21) Papageorgiou, N.; Athanassov, Y.; Armand, M.; Bonhôte, P.; Pettersson, H.; Azam, A.; Grätzel, M. *J. Electrochem. Soc.* **1996**, *143*, 3099.
(22) Matsumoto, H.; Matsuda, T.; Tsuda, T.; Hagiwara, R.; Ito, Y.; Miyazaki, Y. *Chem. Lett.* **2001**, 26.
(23) Kubo, W.; Kitamura, T.; Hanabusa, K.; Wada, Y.; Yanagida, S. *Chem. Commun.* **2002**, 374.
(24) Kubo, W.; Makimoto, Y.; Kitamura, T.; Wada, Y.; Yanagida, S. *Chem. Lett.* **2002**, 948.
(25) Wang, P.; Zakeeruddin, S. M.; Exnar, J.; Grätzel, M. *Chem. Commun.* **2002**, 2972.
(26) Wang, P.; Zakeeruddin, S. M.; Comte, P.; Exnar, J.; Grätzel, M. *J. Am. Chem. Soc.* **2003**, *125*, 1166.
(27) Papageorgiou, N.; Grätzel, M.; Infelta, P. P. *Sol. Energy Mater. Sol. Cells* **1996**, *44*, 405.
(28) Popov, A.; Swemsem, R. F. *J. Am. Chem. Soc.* **1955**, *77*, 3724.
(29) Kopidakis, N.; Schiff, E. A.; Park, N.-G.; van de Lagemaat, J.; Frank, A. J. *J. Phys. Chem. B* **2000**, *104*, 3930.
(30) Nakade, S.; Kambe, S.; Kitamura, T.; Wada, Y.; Yanagida, S. *J. Phys. Chem. B* **2001**, *105*, 9150.
(31) Kambe, S.; Nakade, S.; Kitamura, T.; Wada, Y.; Yanagida, S. *J. Phys. Chem. B* **2002**, *106*, 2967.
(32) Fisher, A. C.; Peter, L. M.; Ponomarev, E. A.; Walker, A. B.; Wijayantha, K. G. U. *J. Phys. Chem. B* **2000**, *104*, 949.
(33) Peter, L. M.; Wijayantha, K. G. U. *Electrochem. Commun.* **1999**, *1*, 576.
(34) Hanabusa, K.; Tange, J.; Taguchi, Y.; Koyama, T.; Shirai, H. *J. Chem. Soc., Chem. Commun.* **1993**, 390.
(35) Hanabusa, K.; Hiratsuka, K.; Kimura, M.; Shirai, H. *Chem. Mater.* **1999**, *11*, 649.
(36) Japanese Industrial Standard Committee. *JAPANESE INDUSTRIAL STANDARD Solar simulators for amorphous solar cells and modules*; Japanese Standards Association: Tokyo, Japan, 1995; Vol. JIS C 8933.
(37) van de Lagemaat, J.; Frank, A. J. *J. Phys. Chem. B* **2001**, *105*, 11194.
(38) Nakade, S.; Saito, Y.; Kubo, W.; Kitamura, T.; Wada, Y.; Yanagida, S. *J. Phys. Chem. B*, submitted.
(39) Schlichthörl, G.; Huang, S. Y.; Sprague, J.; Frank, A. J. *J. Phys. Chem. B* **1997**, *101*, 8141.
(40) Japanese Industrial Standard Committee. *JAPANESE INDUSTRIAL STANDARD Environmental and endurance test methods for amorphous solar cell modules*; Japanese Standards Association: Tokyo, Japan, 1995; Vol. JIS C 8938.
(41) Bonhôte, P.; Dias, A.-P.; Papageorgiou, N.; Kalyanasundaram, K.; Grätzel, M. *Inorg. Chem.* **1996**, *35*, 1168.
(42) Papageorgiou, N.; Barbé, C.; Grätzel, M. *J. Phys. Chem. B* **1998**, *102*, 4156.
(43) Kebede, Z.; Lindquist, S.-E. *Sol. Energy Mater. Sol. Cells* **1998**, *51*, 291.
(44) Tachibana, Y.; Hara, K.; Sayama, K.; Arakawa, H. *Chem. Mater.* **2002**, *14*, 2527.
(45) Japanese Industrial Standard Committee. *JAPANESE INDUSTRIAL STANDARD Secondary reference amorphous solar cells*; Japanese Standards Association: Tokyo, Japan, 1995; Vol. JIS C 8931.
(46) Kubo, W.; Sakamoto, A.; Kitamura, T.; Wada, Y.; Yanagida, S. In preparation.
(47) Buckles, R. E.; Yuk, J. P.; Popov, A. I. *J. Am. Chem. Soc.* **1952**, *74*, 4379.
(48) Loos, K. R.; Jones, A. C. *J. Phys. Chem.* **1974**, *78*, 2306.
(49) Sapp, S. A.; Elliott, M.; Contado, C.; Caramori, S.; Bignozzi, C. A. *J. Am. Chem. Soc.* **2002**, *124*, 11215.
(50) Grätzel, M. *Mesoporous Semiconductor Junctions and Dye Sensitized Solar Cells*; IPS-14; Sapporo, 2002.
(51) Pichot, F.; Gregg, B. A. *J. Phys. Chem. B* **2000**, *104*, 6.